

RESEARCH

Open Access



# Synergistic degradation of Methylene Blue by novel Fe-Co bimetallic catalyst supported on waste silica in photo-Fenton-like system

Khyle Glainmer N. Quiton<sup>1</sup>, Ming-Chun Lu<sup>2</sup> and Yao-Hui Huang<sup>1\*</sup>

## Abstract

In this present study, a novel method to fabricate bimetallic Fe-Co catalyst supported on waste silica was investigated for the photo-Fenton-like (PFL) degradation of Methylene Blue (MB) dye. The uniqueness of this work is on the preparation of the catalyst via fluidized-bed crystallization (FBC) process. Under the optimum conditions of initial pH of 3.0, 3.0 mM of H<sub>2</sub>O<sub>2</sub>, and 1.0 g L<sup>-1</sup> of FBC-derived Fe-Co/SiO<sub>2</sub> catalyst (fFCS), the maximum response for the decoloration and mineralization efficiencies of 20 mg L<sup>-1</sup> of MB in 60 min were 100 and 65%, respectively. Compared to the impregnated Fe-Co/SiO<sub>2</sub> catalyst, the fFCS catalyst exhibited comparable decoloration and mineralization efficiencies, and relatively lower metal leaching for both iron and cobalt. Superoxide radical was unveiled to be the dominant reactive oxygen species in the PFL system over the fFCS catalyst. The catalysts were characterized by Fourier Transform Infrared spectroscopy, Energy Dispersive X-ray spectroscopy and Scanning Electron Microscopy. The results show the successful incorporation of iron and cobalt on the surface of the SiO<sub>2</sub> support material.

**Keywords:** Bimetallic catalyst, Decoloration, Methylene blue, Photo-Fenton-like, Synergistic effect, Waste silica

## 1 Introduction

Advanced oxidation processes (AOPs) have arisen to be effective methods for the degradation and mineralization of recalcitrant organic pollutants including dyes, phenols, surfactants, pesticides, pharmaceuticals existing in industrial wastewaters [1]. These AOPs generate reactive oxygen species (ROS), for instance, highly oxidative and non-selective hydroxyl radical ( $\bullet\text{OH}$ ,  $E_0 = 2.80$  V), less oxidative hydroperoxyl radical ( $\text{HO}_2\bullet$ ,  $E_0 = 1.48$  V), superoxide radical ( $\bullet\text{O}_2^-$ ,  $E_0 = 0.59$  V) and singlet oxygen ( $\text{O}_2^1$ ,  $E_0 = 0.65$  V) [2, 3]. Refractory organics react with these organics and consequently their chemical bonds are annihilated. Accordingly, these recalcitrant

organic compounds are being translated into intermediates and smaller degradation products. These intermediates could be further broken down into carbon dioxide and water by consecutive oxidative reactions under continuous generation of ROS and adequate time [4]. Amongst AOPs, the conventional homogeneous Fenton process is known to be very effectual for the treatment of refractory organic compounds. However, major disadvantages which limit its practical applications comprise: (i) a narrow operating pH range (pH < 3); (ii) a high consumption of hydrogen peroxide (H<sub>2</sub>O<sub>2</sub>); (iii) the generation of an excessive amount of iron-containing sludge; and (iv) relatively high concentrations of iron in the final effluent requiring costly post-treatment process [5]. Correspondingly, modified Fenton processes involving electro-Fenton, photo-Fenton, sono-Fenton, Fenton-like processes, and incorporative processes (combination

\* Correspondence: [yhhuang@mail.ncku.edu.tw](mailto:yhhuang@mail.ncku.edu.tw)

<sup>1</sup>Department of Chemical Engineering, National Cheng Kung University, Tainan 701, Taiwan

Full list of author information is available at the end of the article



© The Author(s). 2022 **Open Access** This article is licensed under a Creative Commons Attribution 4.0 International License, which permits use, sharing, adaptation, distribution and reproduction in any medium or format, as long as you give appropriate credit to the original author(s) and the source, provide a link to the Creative Commons licence, and indicate if changes were made. The images or other third party material in this article are included in the article's Creative Commons licence, unless indicated otherwise in a credit line to the material. If material is not included in the article's Creative Commons licence and your intended use is not permitted by statutory regulation or exceeds the permitted use, you will need to obtain permission directly from the copyright holder. To view a copy of this licence, visit <http://creativecommons.org/licenses/by/4.0/>.

of each) have been developed to surmount these constraints and improve the degradation efficiency. Degradation of methylene blue (MB) using sonophoto-Fenton displayed higher degradation rate ( $0.065 \text{ min}^{-1}$ ) compared to that of  $\text{H}_2\text{O}_2$  + ultraviolet (UV) light irradiation ( $0.030 \text{ min}^{-1}$ ) and  $\text{H}_2\text{O}_2$  + ultrasound (US) irradiation ( $0.015 \text{ min}^{-1}$ ) under similar conditions [6]. Similar results were achieved with the treatment of Congo Red (CR) within 2 h at pH 3 [7].

Cobalt-based catalysts are proficient semiconductor fabric for photocatalytic reaction [8]. Furthermore, these catalysts exhibit excellent catalytic performances for oxidation reactions under acidic and alkaline conditions [8, 9]. Nonetheless, the rapid recombination of electron and hole, and intense light adsorption suppress the photocatalytic efficiency of Co-based catalysts [10]. Additionally, high cobalt leaching has been reported during treatment which leads to secondary environmental pollution [6]. Nevertheless, the strong interaction of cobalt with transition metal ions was found to inhibit the leaching of cobalt from Co-based catalysts [11]. Besides, the  $\text{Co}^{2+}/\text{Co}^{3+}$  redox pair transformation is accelerated and the surface oxygen vacancy generation is improved when a second transition metal is incorporated to Co-containing catalysts [12]. Sun et al. reported that co-doping of Fe with Co onto alumina-mesoporous silica support led to reduced Fe and Co leaching in the reaction system. The leached metal concentrations were recorded as  $21 \mu\text{g L}^{-1}$  for Fe-Co/MCM-41 while that for Fe/MCM-41 and Co/MCM-41 were determined as 64 and  $79 \mu\text{g L}^{-1}$ , respectively [10]. Thus, co-doping of these metals is advantageous to ensure catalyst stability [6]. Moreover, Fe-Co catalysts achieved higher degradation efficiencies compared to their monometallic counterparts [13]. In the photodegradation of MB, CR, and mixed dye (MB + CR), the Fe-Co/ $\text{Al}_2\text{O}_3$ -MCM-41 catalyst showed superior catalytic performance than the supported Fe and Co catalysts indicating an enhanced catalytic activity and performance. Complete degradation of MB was achieved for the supported bimetallic catalyst compared with Fe and Co catalyst achieving 89 and 87% MB degradation, respectively. This superiority in catalytic activity was also evident toward CR degradation achieving 95% for Fe-Co/ $\text{Al}_2\text{O}_3$ -MCM-41 compared with that of Fe/ $\text{Al}_2\text{O}_3$ -MCM-41 reaching about 78% and Co/ $\text{Al}_2\text{O}_3$ -MCM-41 with 75% degradation. Significant synergistic effect was also observed toward the mixed dye showing 100, 93 and 90% for  $\text{Al}_2\text{O}_3$ -MCM-41-supported Fe-Co, Fe and Co catalysts, respectively [14]. CR was also treated using Fe-Co supported on polyacrylamide hydrogel (Fe-Co/PAM) for the activation of hydrogen peroxide reaching 97% efficiency within 60 min. Fe/PAM and Co/PAM showed inferior catalytic

activity compared to Fe-Co/PAM achieving 85 and 85% degradation within 75 min, respectively [13].

In recent years, researchers have been interested in investigating supported catalysts for the catalytic activation of hydrogen peroxide, ozone and peroxymonosulfate for organic pollutant remediation. These catalysts pose advantages such as easy recovery and potential reusability. In some cases, it was reported that supported catalysts exhibit better catalytic activity than the colloidal catalysts [15]. Although nano-sized supported catalysts exhibit improved catalytic activity compared to that of their bulk structures due to change in electronic configuration and sub-surface atomic arrangement, they present difficulty of separation from the treated streams. In addition, nano-sized materials might cause secondary environmental pollution when discharged [16]. Hence, metallic precipitates are infused onto waste silica seed via fluidized-bed crystallization (FBC) and consequently used as catalyst in the photo-Fenton-like (PFL) system. The bimetallic catalysts synthesized from the FBC technology would have a possibility of low moisture content compared to the sludge formed by the traditional precipitation method containing approximately 70% even after filter press dehydration [17]. Su et al. discussed that the solid particles recovered from FBC reactors comprise only of about 1-5% moisture [18]. This leads to no to little cost in post-treatment saving a large amount of sludge treatment cost. The FBC process can possibly simultaneously remove Fe and Co and recover them as bimetallic Fe-Co catalyst. Shih et al. immobilized Mn (II) as manganese dioxide on FeOOH surface via FBC system and utilized the recovered particle to treat arsenic from aqueous solution [19]. The major advantages of FBC over the existing synthesis techniques are the avoidance of sludge formation, material recovery, and reduction of solid wastes. Sludge production is reduced by 75% [20, 21]. Among the current catalyst preparation technologies, impregnation and adsorption/ion exchange are the methods on commercial scale for which impregnation is the most commonly used [22, 23]. On the other hand, plasma technique involved complex processes which leads to difficulty of application on an industrial scale [24]. In addition, reverse micelle (RM) method used on bench scale poses a more complex method in which catalysts are difficult to separate from their constituents. Moreover, catalysts synthesized via RM displays deactivation problem [25]. Added advantages of FBC technique include low operating cost, low operating temperature, use of small amount of chemicals, formation of low moisture content particles and production of more marketable end-product [17].

Herein, a novel approach to fabricate Fe-Co bimetallic catalyst supported on waste silica (Fe-Co/ $\text{SiO}_2$ ) is reported to act as a PFL catalyst to treat MB in aqueous

solutions. To our knowledge, there have been no reports on the preparation of Fe-Co/SiO<sub>2</sub> via FBC process. This novel technology was utilized as a catalyst synthesis method without compromising effluent standards. The catalytic performance of this catalyst was compared with that of the catalyst synthesized via a common synthesis technique, incipient wetness impregnation, to determine its efficacy and feasibility for practical applications.

## 2 Materials and methods

### 2.1 Chemicals

All chemicals in this study were of reagent grade and used as received without further purification. Cobalt sulfate heptahydrate (CoSO<sub>4</sub>·7H<sub>2</sub>O, 99%) was purchased from Sigma-Aldrich (China). Hydrogen peroxide (H<sub>2</sub>O<sub>2</sub>, 30% w/v) and iron sulfate heptahydrate (CoSO<sub>4</sub>·7H<sub>2</sub>O, 99%) were supplied by Panreac (Germany). Sodium hydroxide (NaOH, ≥ 97%) was obtained from Fisher Chemical (UK). Sulfuric acid (H<sub>2</sub>SO<sub>4</sub>, 98%), ammonium oxalate monohydrate ((NH<sub>4</sub>)<sub>2</sub>C<sub>2</sub>O<sub>4</sub>·7H<sub>2</sub>O, ≥ 99.5%), and sodium sulfate (Na<sub>2</sub>SO<sub>4</sub>, ≥ 99%) were purchased from Honeywell (Germany). Tert-butyl alcohol ((CH<sub>3</sub>)<sub>3</sub>COH, 99.5%) and furfuryl alcohol (C<sub>5</sub>H<sub>6</sub>O<sub>2</sub>, 98%) were supplied by Merck (Germany) and Acros Organics (USA), respectively. Silica support material with 0.5–0.7 mm particle size was obtained as a waste from Chang-Chun Petrochemical, Taiwan. For all the experiments, deionized water was supplied by a laboratory-grade RO-ultrapure water system (resistance > 18.1 Ω).

### 2.2 Preparation of Fe-Co/SiO<sub>2</sub> catalyst by FBC

The bimetallic catalyst was prepared by FBC, and CoSO<sub>4</sub>·7H<sub>2</sub>O and FeSO<sub>4</sub>·7H<sub>2</sub>O were used as metal precursors. A 280-ml fluidized-bed reactor (FBR) with a height of 1 m shown in Fig. 1 was used to prepare the catalyst. 2-mm glass beads were placed inside the FBR occupying a height of 2 cm to provide a stable settling bed for the support material and then the SiO<sub>2</sub> support was loaded with a static bed height of 10 cm to ensure uniform incorporation of iron and cobalt on the support surface. Specific amounts of metal precursors with an Fe to Co molar feeding ratio of 1:1 and carbonate solution with carbonate to metal ratio of 1.2:1 were supplied to the reactor at a constant flow rate of 5 mL min<sup>-1</sup> using an input peristaltic pump (Masterflex) to cause the SiO<sub>2</sub> bed to be fluidized. Using a recirculation peristaltic pump (Masterflex), the reaction solutions were reintroduced to the bottom of the reactor at a reflux rate of 300 mL min<sup>-1</sup> to maintain at least 50% bed expansion providing fluidization, and thus, incorporating the iron and cobalt in the SiO<sub>2</sub> surface. Catalyst synthesis by FBC was done at room temperature and was conducted for 4 h ensuring no iron and cobalt residue in the effluent. The Fe-Co catalyst supported by waste silica synthesized

via FBC is designated as fFCS. Fe/SiO<sub>2</sub> (FS) and Co/SiO<sub>2</sub> (CS) were fabricated using an analogous procedure for comparison purposes.

### 2.3 Preparation of fFCS by impregnation

The contrastive bimetallic catalyst was fabricated by incipient wetness co-impregnation with the same precursors and Fe to Co molar feeding ratio. Before impregnation, the support material SiO<sub>2</sub> was oven-dried at 60 °C overnight. The metal precursors were then dissolved in 800 mL of deionized water in a 1-L beaker and the waste silica was progressively added to the solution under intense stirring. Subsequently, the solution was heated at 85–90 °C to vaporize the excess water. Consequently, the material was oven-dried at 60 °C overnight. The dried material was then calcined at 400 °C for 4 h in a muffle furnace. The catalyst synthesized by impregnation technique is designated as iFCS.

### 2.4 PFL degradation of MB dye

A 1.5-L three-phase FBR (3P-FBR) was used to carry out the PFL degradation experiments at room temperature under UV-A light illumination as shown in Fig. 2. Three phases involved in the 3P-FBR are liquid, solid and air in which excellent contact among the reactants coupled with high mass and heat transfer rates are achieved. The cylindrical reactor was made of Pyrex glass comprised of a diameter of 8 cm and height of 44 cm with a membrane air diffuser at the bottom part. A 36-W mercury lamp with a wavelength of 365 nm (Philips, Poland) was positioned at the center of the reactor to achieve uniform light irradiation of 1.45 × 10<sup>-9</sup> W cm<sup>-2</sup> throughout the 0.06 mM (20 mg L<sup>-1</sup>) MB solution. The initial pH of the solution was adjusted using H<sub>2</sub>SO<sub>4</sub> and NaOH. Consequently, the catalyst and H<sub>2</sub>O<sub>2</sub> were added sequentially to start the catalytic reaction. The catalyst added in a 1 L of MB solution was fluidized by introducing air bubbles from the bottom of the reactor unto the system with the aid of an aeration pump at 6 × 10<sup>-3</sup> m<sup>3</sup> min<sup>-1</sup> flow rate. Samples were drawn from the reactor at specified time interval and filtered using a 0.22 μm syringe filter. The chemical reaction was quenched by adding a few drops of 1 M NaOH to the sample to raise the pH to about 9.0 before analysis.

The effects of different reaction parameters were also assessed in this work. Specifically, the initial pH (pH<sub>i</sub>) was adjusted between 2.0 and 9.0. In addition, The H<sub>2</sub>O<sub>2</sub> dosage and catalyst loading was set from 0.5 to 10 mM and 0.25 to 2.0 g L<sup>-1</sup>, respectively. To evaluate the catalytic performance of iFCS compared with that of fFBC, same procedure was applied as mentioned above. The decoloration of MB was calculated using the following equation:

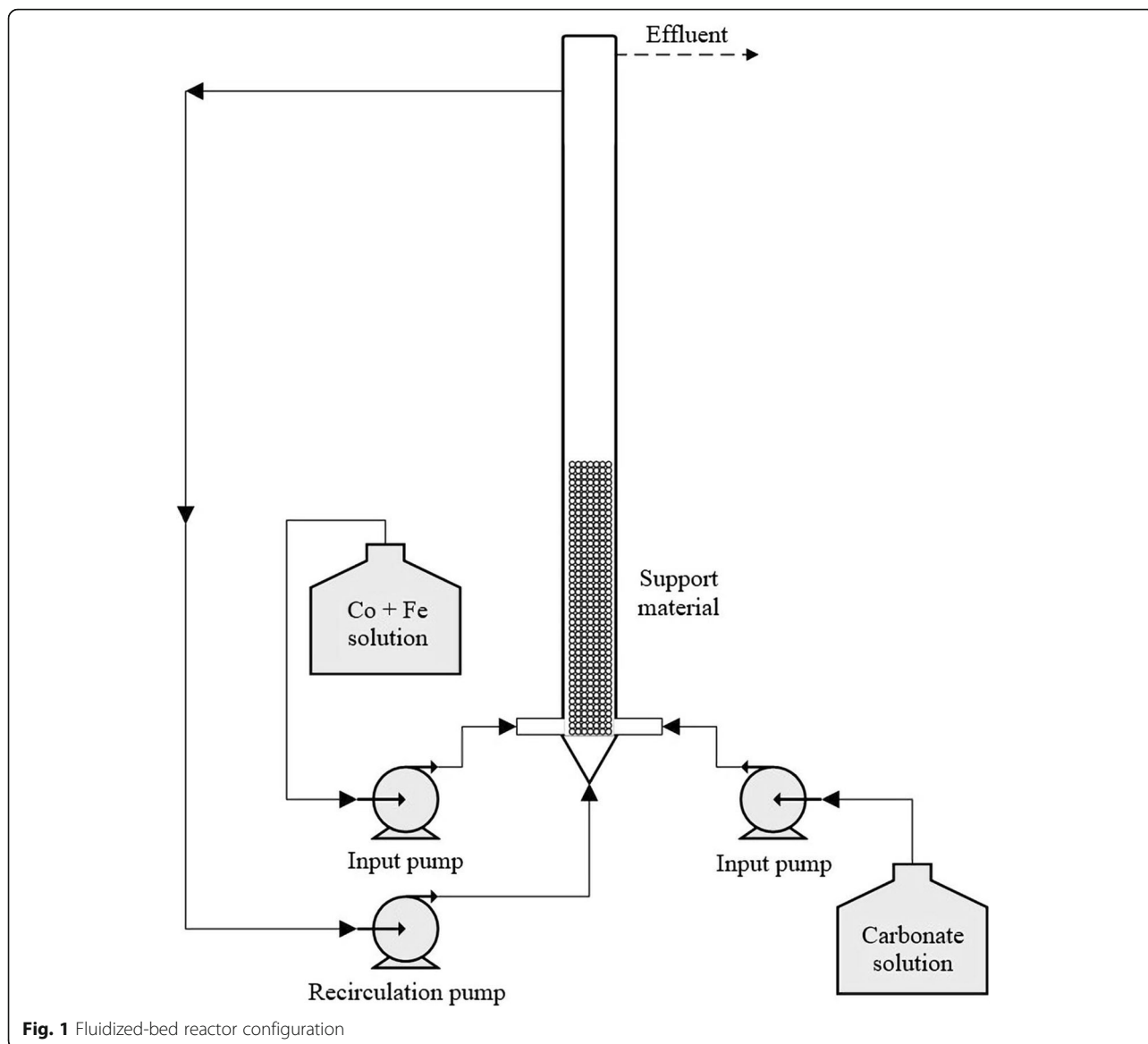


Fig. 1 Fluidized-bed reactor configuration

$$\begin{aligned} \text{Decoloration efficiency (\%)} \\ = \left(1 - \frac{MB_R}{MB_i}\right) \times 100 \end{aligned} \tag{1}$$

where  $MB_i$  and  $MB_R$  are the initial and residual concentration after treatment, respectively.

The MB decoloration rate was fitted with the pseudo-first order kinetic model. The rate constant for the decoloration of MB dye was determined from:

$$\ln\left(\frac{MB_i}{MB_R}\right) = kt \tag{2}$$

where  $MB_i$  and  $MB_R$  are the initial and residual concentration at operating time  $t$ , respectively, and  $k$  is the apparent pseudo-first order rate constant. Additionally, the

mineralization efficiency of MB is given by the following equation:

$$\begin{aligned} \text{Mineralization efficiency (\%TOC}_r\text{)} \\ = \left(1 - \frac{TOC_R}{TOC_i}\right) \times 100 \end{aligned} \tag{3}$$

where  $TOC_i$  and  $TOC_R$  are the initial and residual total organic carbon content after treatment, respectively.

### 2.5 Evaluation of active species

Tert-butyl alcohol (TBA), furfuryl alcohol (FFA), ammonium oxalate monohydrate (AO), and sodium sulfate (SS) were used as hydroxyl radical, superoxide radical, hole and electron pair scavengers, respectively. Briefly, a specific amount of the chosen radical scavengers was

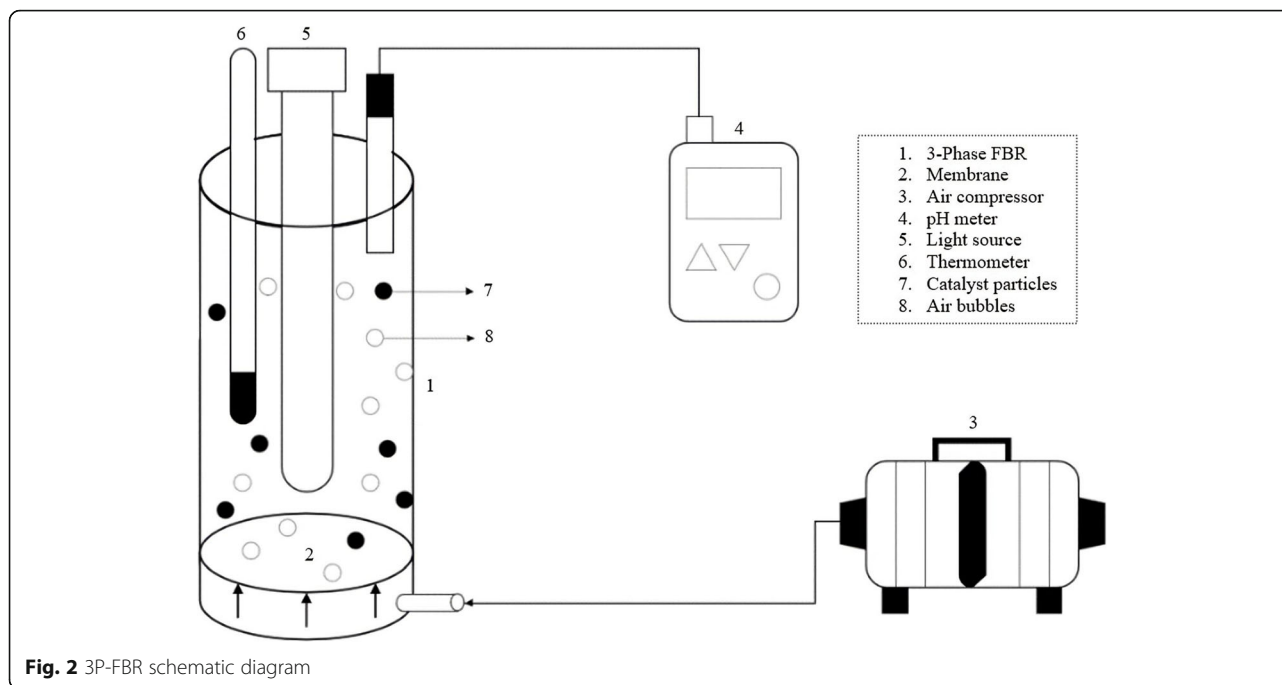


**Fig. 2** 3P-FBR schematic diagram

added to the MB solution. Before illumination, the solution was stirred intensively until it reached homogeneity. The PFL catalytic degradation steps are similar with the procedure described in the previous section (Section 2.4). The scavenging efficiency was estimated as follows [26]:

$$\text{Scavenging efficiency (\%)} = \left(1 - \frac{k_{RS}}{k_{PFL}}\right) \times 100 \quad (4)$$

where  $k_{RS}$  and  $k_{PFL}$  are the pseudo first-order rate constants for the decoloration of MB in the presence and absence of radical scavengers.

### 2.6 Analytical methods

Absorbance of MB dye at 664 nm and absorbance of residual  $H_2O_2$  at 405 nm were analyzed using a diode array UV-Vis spectrophotometer (Agilent 8453, USA). Residual  $H_2O_2$  was determined by Titanium Sulfate Method.  $H_2O_2$  efficiency refers to the percentage of  $H_2O_2$  remaining in the reaction system as described by Eq. (5). The TOC content was determined using TOC analyzer (Siever 900 Innovox, General Electric Company, USA). Iron and cobalt residues were measured by using inductively coupled plasma mass spectrometry (JY 2000-2, HORIDA).

$$H_2O_2 \text{ efficiency (\%)} = \frac{H_R}{H_i} \times 100 \quad (5)$$

where  $H_R$  and  $H_i$  are the residual and initial  $H_2O_2$  concentrations in mM, respectively.

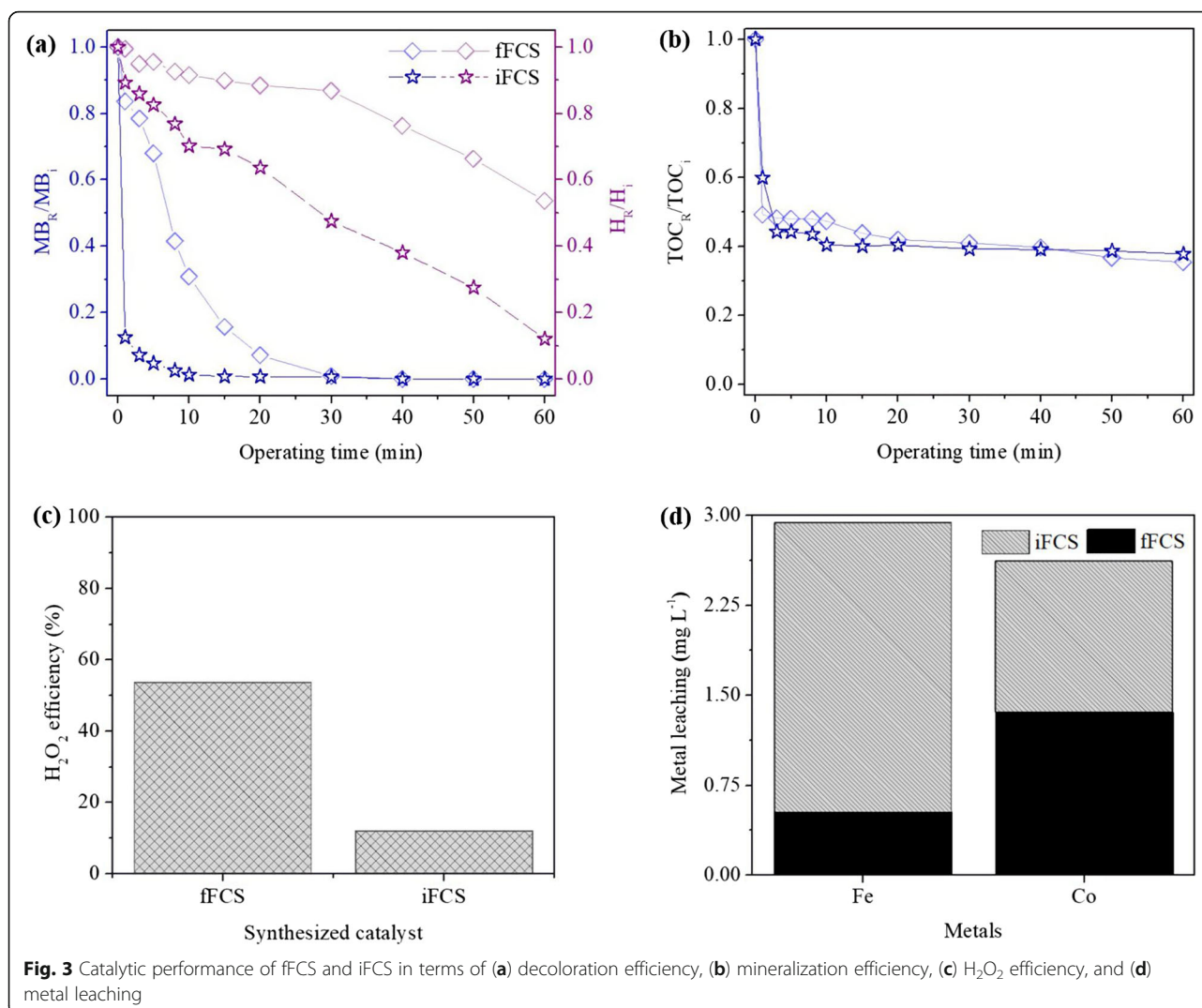
### 2.7 Catalyst Characterization

Fourier transform infrared spectroscopy (FTIR, Thermo Scientific Nicolet 6700, USA) was used to determine the surface compound. Scanning electron microscope (SEM, JSM-6700 F, JEOL) at 10 kV and 7 mA integrated with an energy dispersive spectroscopy (EDS, INCA400, OXFORD) was employed to observe the morphological features and the elemental composition of the catalysts.

## 3 Results and discussion

### 3.1 Catalytic performance of fFCS and iFCS

To assess the feasibility of FBC as a novel technique to prepare bimetallic Fe-Co catalyst for industrial and engineering applications, contrastive bimetallic Fe-Co catalyst was synthesized via incipient wetness impregnation and their catalytic performances are displayed in Fig. 3. The decoloration rate of MB using iFCS was extremely fast achieving almost complete decoloration (99%) within 15 min which may be ascribed to the quick  $H_2O_2$  consumption in the PFL reaction system as seen in Fig. 3a. Meanwhile, the mineralization efficiencies for both catalysts utilized are almost similar reaching 65 and 62% for fFCS and iFCS, respectively (Fig. 3b). Fe-Cu supported on ZSM-5 prepared by hydrothermal and ion-exchange methods showed different degradation efficiencies toward Rhodamine 6G dye [27]. Catalytic performance of bimetallic catalysts is typically in relation with the catalyst preparation method. At present, methods utilized in the chemical industry are limited because of raw materials cost, and storage, transportation, and large-scale production limitations [28]. In this present



work, it can be divulged that the photocatalytic activity and performance of the iFCS catalyst prepared via FBC is comparable with that of a common synthesis method, incipient wetness impregnation. Thus, fFCS was further investigated not only considering the comparable MB decoloration and mineralization efficiencies but also the synthesis time and operating temperature of the catalyst preparation process. The impregnation technique used in this study was operated for 12 h at 85-90 °C to vaporize the excess water which shows longer synthesis time and higher operating temperature compared to that of the FBC technique (4 h under room temperature).

### 3.2 Catalyst characterization

FTIR analysis was employed to demonstrate the successful incorporation of Fe and Co unto the waste silica scaffold. As presented in Fig. 4a, the absorption peaks centered at 453, 814 and 1082  $cm^{-1}$  are ascribed to the Si-O-Si bending, asymmetric and symmetric stretching

vibrations, respectively [6]. The band positions of fFCS are almost similar with that of  $SiO_2$  which suggests that the metal oxide incorporation on the surface of  $SiO_2$  had no significant effect on the Si-O-Si bond as shown in Fig. 4a and b. The band peaks at 1622 and 3400-3402  $cm^{-1}$  describe the deformation vibration of adsorbed  $H_2O$  and the O-H stretching of both adsorbed  $H_2O$  molecules and H-bonded surface silanol groups in the  $SiO_2$  matrix. Additionally, characteristic peaks from 400 to 700  $cm^{-1}$  indicated in Fig. 4b and c refer to magnetite,  $Fe_3O_4$ , in agreement with the illustrated peaks in this range as the main band representing the iron oxide existence [29]. For fFCS, a characteristic band at 619  $cm^{-1}$  is ascribed to the Fe-O stretching vibrations [30]. The FTIR spectrum of  $Co_3O_4$  indicates characteristic absorption bands at 605 and 690  $cm^{-1}$  for iFCS and fFCS, respectively. It was reported that the bands at very near values of 607 and 694  $cm^{-1}$  refers to the infrared spectrum of the  $Co_3O_4$  spinel. JirátoVá et al. affirmed the

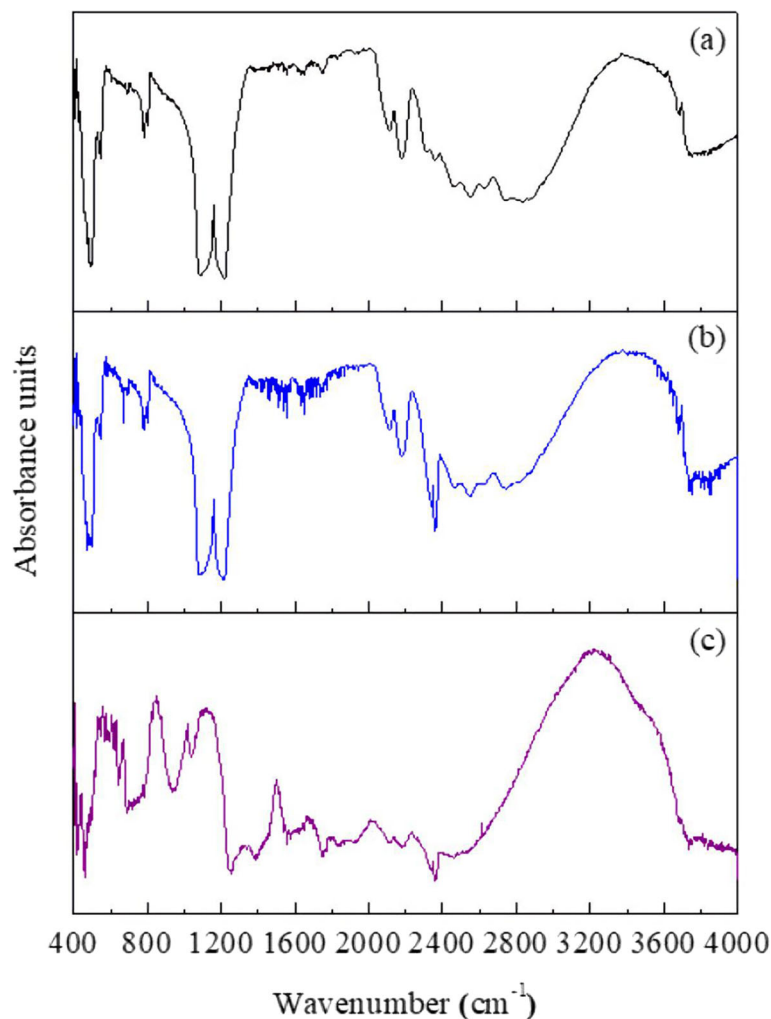
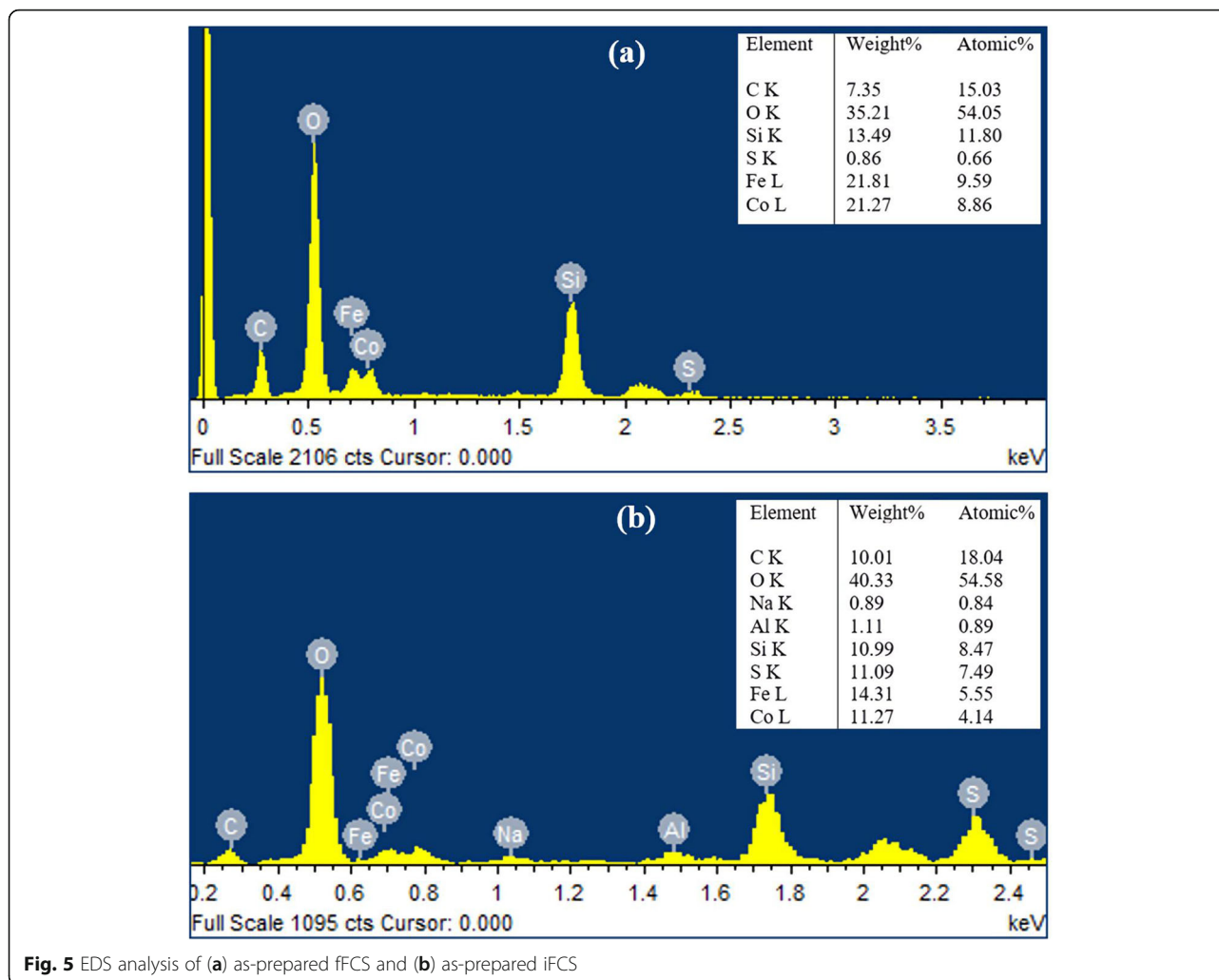


**Fig. 4** FTIR spectra of (a) SiO<sub>2</sub> support, (b) as-prepared fFCS and (c) as-prepared iFCS

appearance of Co<sub>3</sub>O<sub>4</sub> at the band of 694 cm<sup>-1</sup> for the spectrum of Co-RF-1 sample [31]. EDS analysis also indicated the incorporation of Fe and Co unto the SiO<sub>2</sub> surface as shown in Fig. 5. fFCS catalyst exhibited 21.8% Fe and 21.3% Co content (Fig. 5a) while iFCS contains 14.3% Fe and 11.3% Co (Fig. 5b) which resulted to the molar ratio of Fe to Co to be about 0.39:0.38 and 0.26:0.19, respectively. These results clearly affirmed the successful fabrication of fFCS and iFCS catalysts showing the effective incorporation of the metal oxides on the waste silica surface. Moreover, the surface of fFCS exhibits a smoother surface (Fig. 6c, d) compared to the SiO<sub>2</sub> surface (Fig. 6a, b) which possibly indicates the successful incorporation of iron and cobalt into the SiO<sub>2</sub> framework. Contrariwise, the morphological feature of iFCS became rather rougher than the fFCS catalyst surface which also possibly reveals clusters of metal oxides outside the SiO<sub>2</sub> structures (Fig. 6e, f).

### 3.3 Catalytic activity of fFCS

The catalytic performance of the FBC-derived catalyst was investigated by the photocatalytic degradation of MB solution under UV-A light irradiation and the results are indicated in Fig. 7. In the absence of H<sub>2</sub>O<sub>2</sub> and Fe-Co/SiO<sub>2</sub> catalyst, simply 16% MB degradation efficiency with the decoloration rate attaining 0.0016 min<sup>-1</sup> was reached under UV-A light irradiation within 60 min of reaction as shown in Fig. 3a. This indicates that the photolysis degradation was very weak. Photocatalysis removed 20% of MB dye in the reaction system with a decoloration rate of 0.0021 min<sup>-1</sup>. While only 6% MB was degraded using only Fe-Co/SiO<sub>2</sub> which shows weak adsorption ability. Using the H<sub>2</sub>O<sub>2</sub> system, MB was removed by 15%. The UV-A light and H<sub>2</sub>O<sub>2</sub> process was also performed to accomplish outstanding decoloration efficiency. Using UV-A/H<sub>2</sub>O<sub>2</sub> system, 34% MB was degraded within 60 min. H<sub>2</sub>O<sub>2</sub> in



combination with light illumination leads to enhanced catalytic activity which is caused by the generation of hydroxyl radicals [32]. Fenton-like process achieved 69% decoloration efficiency showing an appreciable activity with the use of the heterogeneous catalyst even under dark condition. Furthermore, it was found that the PFL system using Fe-Co/SiO<sub>2</sub> catalyst achieved 99% attaining a  $k$  value of 0.065 min<sup>-1</sup> within 60 min of operation time which showed that the catalyst used presented a good catalytic activity and could respond to H<sub>2</sub>O<sub>2</sub> to generate •OH radicals to degrade MB. UV light illumination enhances Fe<sup>3+</sup> to Fe<sup>2+</sup> reduction in the solution and more •OH radicals are generated during the degradation process. The generated Fe<sup>2+</sup> reacts again with H<sub>2</sub>O<sub>2</sub> leading to production of new •OH radicals [4]. Likewise, H<sub>2</sub>O<sub>2</sub> is decomposed to generate additional •OH radicals under UV light irradiation via photolysis [4]. The pseudo-first order rate constants of MB decoloration are presented in Fig. 7b. The

decoloration rates obtained for different processes were consistent with the results obtained from the MB decoloration. The decoloration efficiency of MB followed this sequence: UV + H<sub>2</sub>O<sub>2</sub> + FCS > H<sub>2</sub>O<sub>2</sub> + FCS > UV + H<sub>2</sub>O<sub>2</sub> > UV + FCS > UV > H<sub>2</sub>O<sub>2</sub> > FCS. Moreover, the enhancement of the photocatalytic MB degradation efficiency in the reaction system was brought about by the incorporative effect of photocatalysis and simultaneous Fenton-like process [7]. Significantly, the decoloration rate of the synergistic process is about 31-fold that of PC process alone and 4-fold that of Fenton-like process alone which could be attributed to the combined influence of both processes. From Fig. 7b, it is observable that the apparent decoloration rate of the PFL process was greatly enhanced compared to the single processes. The contributory effects of the photocatalytic process and the Fenton-like reaction to the PFL process were explored using the synergy index described as the ratio of the PFL catalytic rate constant to the sum of the rate constants of the single processes given by the Eq. (6) [7]:

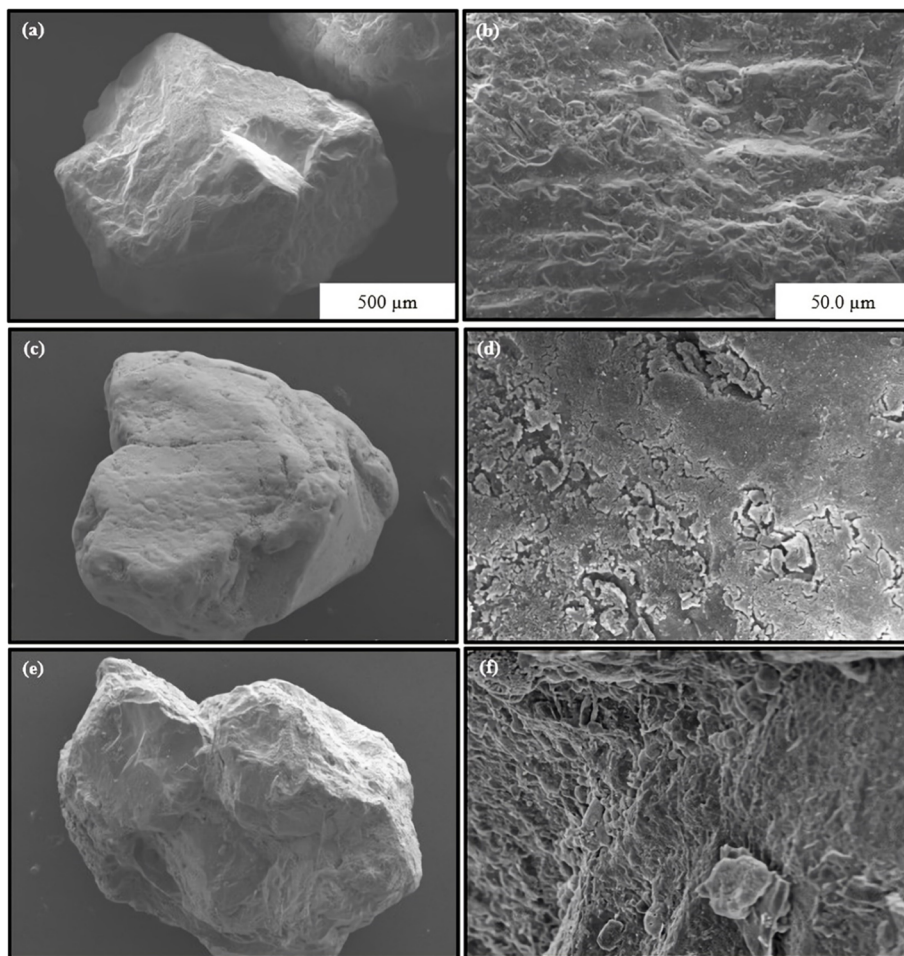


**Fig. 6** SEM images of (a, b) SiO<sub>2</sub> support, (c, d) as-prepared fFCS and (e, f) as-prepared iFCS (left: 500 μm; right: 50.0 μm)

$$\text{Synergy index} = \frac{k_{\text{PFL}}}{k_{\text{PC}} + k_{\text{FL}}} \quad (6)$$

where  $k_{\text{PFL}}$ ,  $k_{\text{PC}}$  and  $k_{\text{FL}}$  are the apparent decoloration rates of PFL, photocatalysis and Fenton-like processes in  $\text{min}^{-1}$ , respectively. The synergy index value for the MB decoloration by PFL process under UV-A irradiation is 3.8 which indicates a good synergy between photocatalysis and Fenton-like processes (greater than 1.0). This may be ascribed to (i) the increase in active species needed in the decoloration process generated due to UV-A light irradiation, (ii) the improved transfer of active species from the liquid to the solid interface, and (iii) the activation of the catalyst with H<sub>2</sub>O<sub>2</sub> generating required active species in the reaction system.

### 3.4 Enhanced catalytic performance of fFCS

The degradation of MB via H<sub>2</sub>O<sub>2</sub> activation with FBC-synthesized FS, CS and Fe-Co/SiO<sub>2</sub> was further comprehensively assessed (Fig. 8). FS and CS could substantially

degrade MB by 92 and 89%, respectively, as indicated in Fig. 8a. The catalytic activity of FCS is comparable to that of FS even though the active cobalt is halved due to iron replacement in the catalyst suggesting a synergistic effect of Fe and Co in terms of MB decoloration. In terms of mineralization (Fig. 8b), the addition of Fe into Co increased its mineralization efficiency reducing the initial TOC content of 21 mg L<sup>-1</sup> by 56%. Even though higher amount of H<sub>2</sub>O<sub>2</sub> to treat the MB pollutant was consumed (Fig. 8c), FCS showed greater stability in terms of Fe and Co leaching in the system (Fig. 8d). The leaching of Fe and Co by FCS was reduced by 24 and 62% compared to FS and CS, respectively, implying the inhibitory effect of adding Fe into Co and vice versa. Farias et al. affirms the problem of metal leaching of cobalt-based catalysts during the degradation process and secondary environmental pollution is possible [33]. It was reported that the inhibition of cobalt leaching from cobalt-based catalysts could be aided by the strong interaction of cobalt to transition metal ions [34]. Furthermore, the transformation of Co<sup>3+</sup>/Co<sup>2+</sup> redox pair

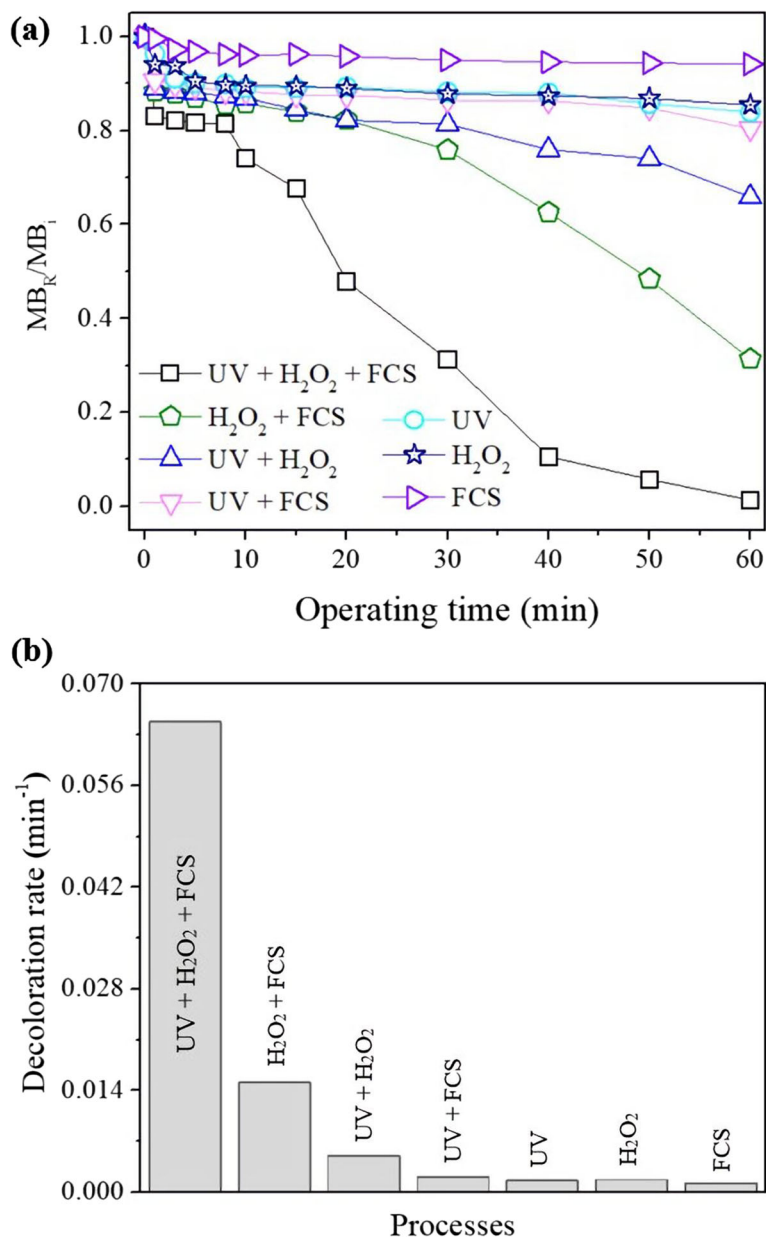


**Fig. 7** Degradation of MB under different processes ( $[MB]_i = 0.06$  mM;  $[H_2O_2]_i = 1.5$  mM;  $pH_i = 3.0$ ; cat. dose =  $0.85$  g L<sup>-1</sup>; air flow rate =  $6 \times 10^{-3}$  m<sup>3</sup> min<sup>-1</sup>; UV = 365 nm)

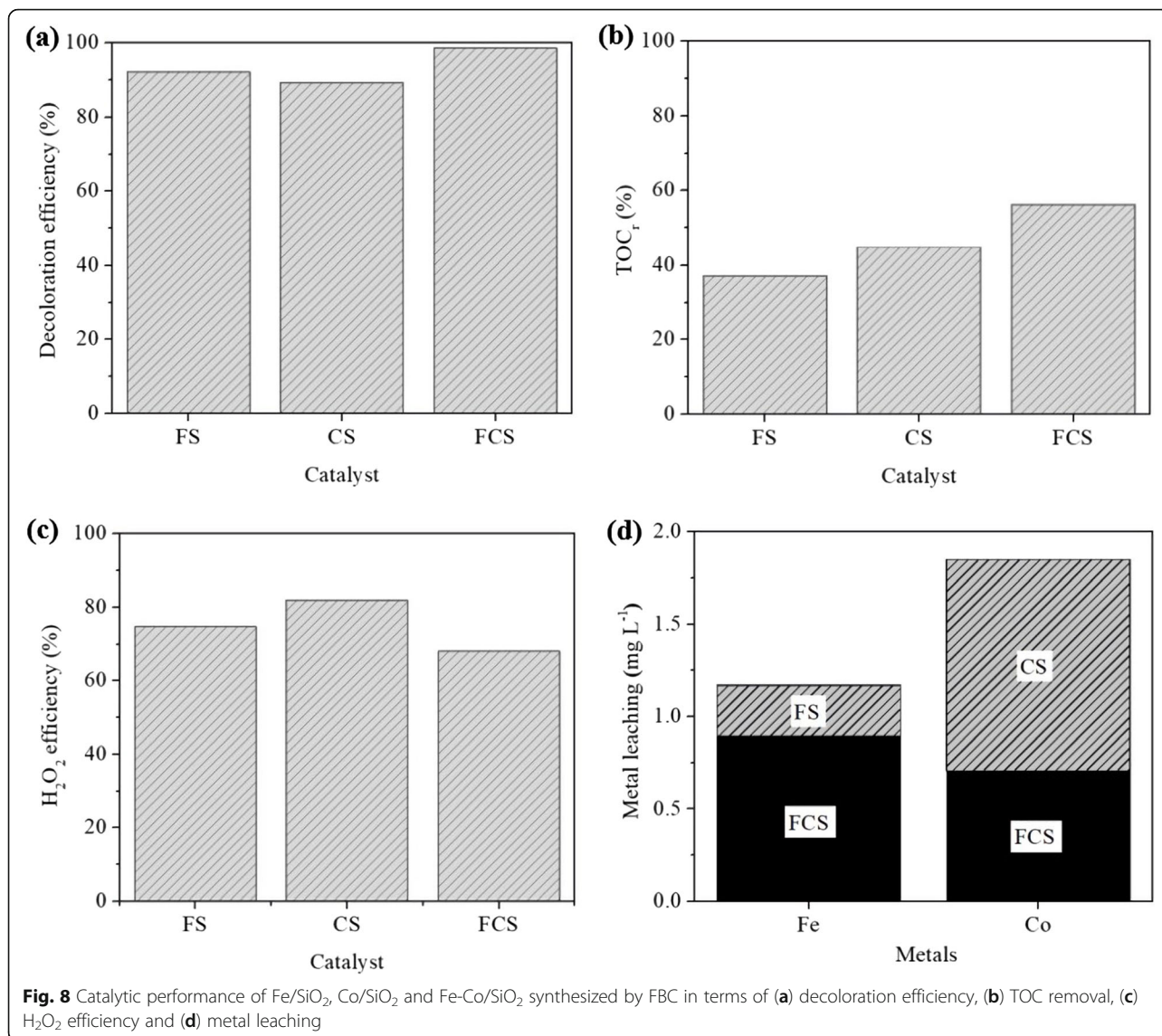
could be accelerated and the production of surface oxygen vacancies could be improved with the addition of a second metal unto cobalt-containing catalysts [12]. Incorporating Fe into Co supported by waste silica improved the photocatalytic activity and stability of the heterogeneous catalyst in the PFL system. Hence, Fe-Co co-doping is advantageous to ensure catalytic stability. The difference in MB decoloration and mineralization efficiencies achieved using the bimetallic catalyst and its monometallic counterparts greatly implied a synergistic

effect between iron and cobalt via oxidation-reduction reaction.

### 3.5 PFL degradation of MB

#### 3.5.1 Effect of initial pH

The effect of initial pH on decoloration of MB in UV-A + H<sub>2</sub>O<sub>2</sub> + fFCS system is presented in Fig. 9 ranging from 2.0 to 9.0. The pH of the solution has a critical influence on MB degradation because it controls the catalytic activity resulting in iron ions and H<sub>2</sub>O<sub>2</sub> stability [34]. Previous studies have presented favorable



photodegradation occurring at low pH value. It was concluded by Vinita et al. that solution pH greatly hampers in hydroxyl radical formation and in organic compound oxidation [35]. Moreover, an acidic environment improves the generation of oxidative radicals leading to enhanced oxidation of organic substrate. At pH value of 3.0, UV-A and visible solar light illumination favorably lead to the formation of the most photo-active Fe<sup>3+</sup>-hydroxyl complex, Fe(OH)<sup>2+</sup> [36]. MB degradation was comparatively slower and lower at pH<sub>i</sub> 2.0 which could be accredited to protonating H<sub>2</sub>O<sub>2</sub> and disadvantaging the formation of •OH radical [37]. The decrease in MB decoloration when the initial pH decreased from 3.0 to 2.0 could also be attributed to the production of [Fe<sup>II</sup>(H<sub>2</sub>O)]<sup>2+</sup> generating hydroxyl radicals with lesser reactivity. In addition, the hydroxyl radical scavenging effect could have taken place (Eq. (7)) and oxonium ions

([H<sub>3</sub>O<sub>2</sub>]<sup>+</sup>) could have possibly formed from H<sub>2</sub>O<sub>2</sub> at lower pH (Eq. (8)). These oxonium ions also probably generate more stable H<sub>2</sub>O<sub>2</sub> in the reaction system and hindered its activity with ferric ions [38].



In the present work, the optimal initial pH was observed to be 3.0 in which the maximum MB decoloration was achieved within 60 min. Ahmed et al. affirms that the optimum pH to treat 0.06 mM (20 mg L<sup>-1</sup>) MB dye was 3.0 using 3.0 mM of H<sub>2</sub>O<sub>2</sub> dosage and 0.85 g L<sup>-1</sup> of SiO<sub>2</sub>-supported Fe-Ni catalyst using visible light source [38]. The point of zero charge (pH<sub>pzc</sub>) of fFCS could possibly be around 1.8-4.2 due to the presence of

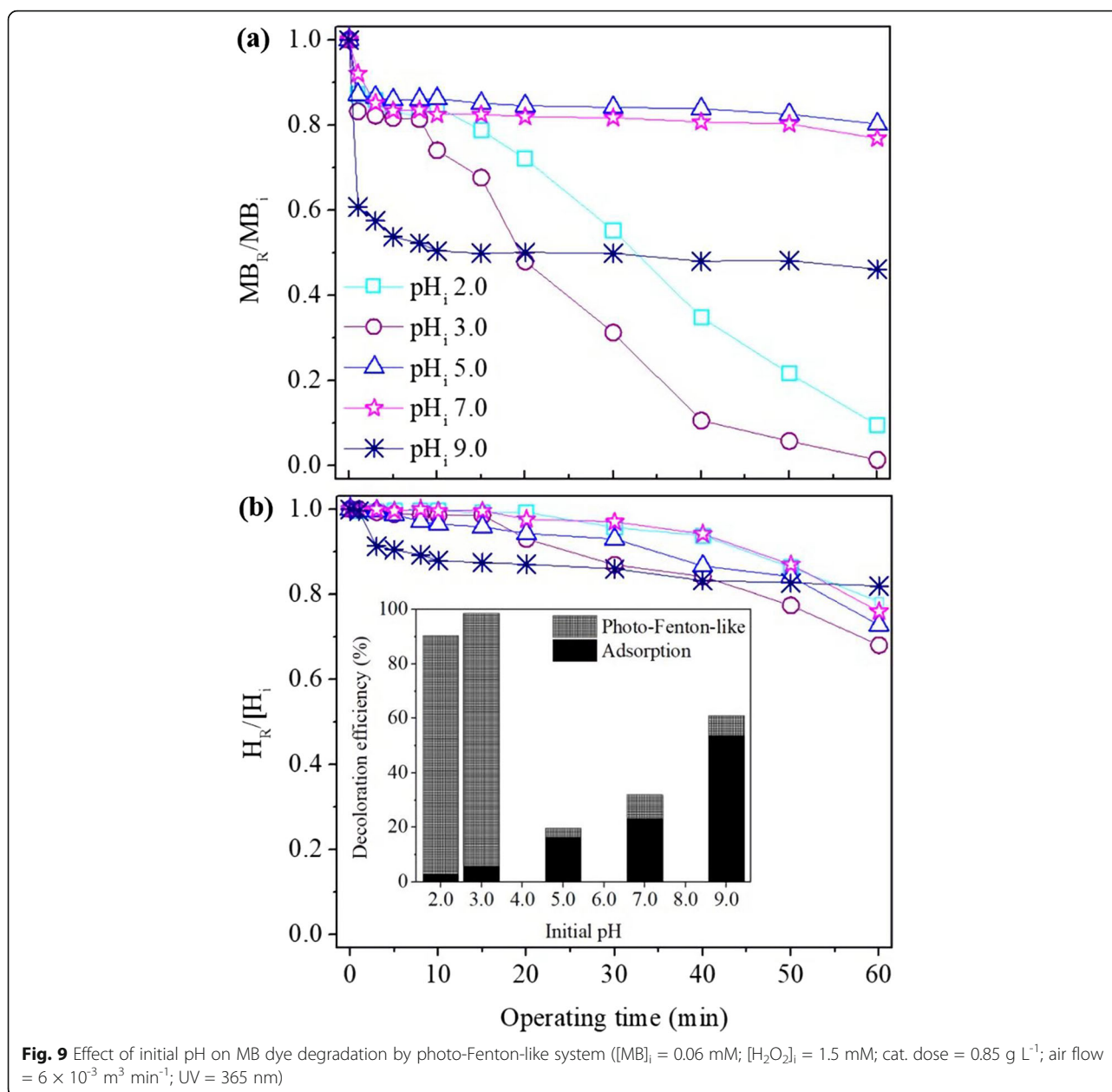
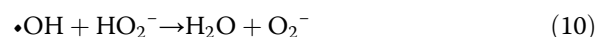
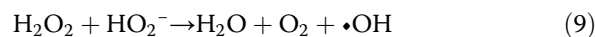


**Fig. 9** Effect of initial pH on MB dye degradation by photo-Fenton-like system ( $[MB]_i = 0.06$  mM;  $[H_2O_2]_i = 1.5$  mM; cat. dose =  $0.85$  g  $L^{-1}$ ; air flow =  $6 \times 10^{-3}$  m<sup>3</sup> min<sup>-1</sup>; UV = 365 nm)

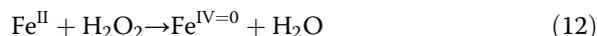
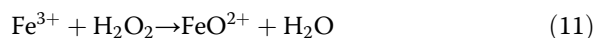
SiO<sub>2</sub> [39]. At higher pH value ( $pH > 4.2$ ), the surface of fFCS would be negatively charged, hence the adsorption of the cationic MB dye via  $\pi$ - $\pi$  stacking and electrostatic attraction is favorable as seen in Fig. 9b. The negatively charged surface of the catalyst could be attributed to silicic surface formation via interfacial dissociation of silanol groups [38]. As the pH increased from 5.0 to 9.0, the electrostatic interaction between the surface of the catalyst and the MB dye could become greater leading to higher MB decoloration in the reaction system due to adsorption phenomenon. Furthermore, the reduced oxidation effectiveness and decrease in  $H_2O_2$  concentration at this pH range could be caused by auto-decomposition

of additional  $H_2O_2$  into  $H_2O$  and  $O_2$ , and not into  $\bullet OH$  radical with great potential for oxidation due to instability of  $H_2O_2$  at higher pH level [40]. In addition,  $H_2O_2$  can react with  $OH^-$  leading to generation of oxidizing species hydroperoxyl anion ( $HO_2^-$ ) reducing the  $H_2O_2$  concentration [41]. The anion  $HO_2^-$  can interact with both  $H_2O_2$  and  $\bullet OH$  radical given by the following:



On top of that, the reduction of catalytic activity at elevated pH value leading to remarkable decrease in

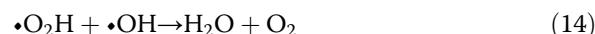
decoloration rate can possibly be ascribed to the generation of relatively inactive ferryl ions ( $\text{FeO}^{2+}$ ) as shown in Eq. (11). Under basic conditions, generation of high-valent iron species,  $\text{Fe}^{\text{IV}=\text{O}}$ , may also occur which is less reactive than  $\bullet\text{OH}$  radicals indicated in Eq. (12).



### 3.5.2 Effect of $\text{H}_2\text{O}_2$ dosage

In the PFL process,  $\text{H}_2\text{O}_2$  plays a crucial role in the dye degradation, therefore the optimization of  $\text{H}_2\text{O}_2$  dosage in the reaction system is a significant parameter for achieving maximum MB dye degradation. Figure 10 shows the impact of  $\text{H}_2\text{O}_2$  dosage on the MB dye degradation efficiency in UV-A +  $\text{H}_2\text{O}_2$  + fFCS system. To observe the behavior of the reaction system over a wide  $\text{H}_2\text{O}_2$  dosage range, experimental runs were conducted from 0.5 to 10 mM of  $\text{H}_2\text{O}_2$ . The decoloration rate of MB was accelerated with increasing  $\text{H}_2\text{O}_2$  amount from 0.5 to 3.0 mM leading to decoloration efficiency from 80 to 99%. The results presented are in agreement with the general trend [42]. The increase in decoloration efficiency is attributable to the generation of additional  $\bullet\text{OH}$  radicals in the reaction process [5]. Even so, exceeding this value leads to unfavorable effect. The degradation rate increased negligibly with increase in  $\text{H}_2\text{O}_2$  dosage from 3.0 to 10.0 mM which may be accredited to the scavenging activity of excess  $\text{H}_2\text{O}_2$  (Eq. (13)) and

generation of  $\bullet\text{OH}$  radicals which acts as  $\bullet\text{OH}$  radical scavengers (Eq. (14)) reducing the availability of  $\bullet\text{OH}$  and consequently lowering the decoloration efficiency [42]. Meanwhile, as the MB molecules saturate the catalyst active sites the extra MB molecules in the medium can function as radical scavengers decreasing the degradation rate [43]. In addition, the  $\bullet\text{O}_2\text{H}$  radicals exhibit much lower oxidation capability than  $\bullet\text{OH}$  radicals which could have resulted in lower MB degradation efficiency in the PFL system.



### 3.5.3 Effect of catalyst loading

Figure 11 presents the impact of catalyst loading on the efficiency of MB dye degradation in UV-A +  $\text{H}_2\text{O}_2$  + fFCS system. The decoloration rate of MB was significantly affected by the catalyst loading during the degradation process. Increase in catalyst loading aids in producing additional  $\bullet\text{OH}$  radicals which might also interact with themselves resulting in subsequent quenched reaction [44]. Moreover, it produces more turbidity and high opacity in the solution on account of a higher catalyst dosage leading to difficulty of light infiltration [45]. Increase in catalyst loading led to an improved decoloration efficiency (Fig. 11a) owing to the probable increase in the catalytic active surface sites and

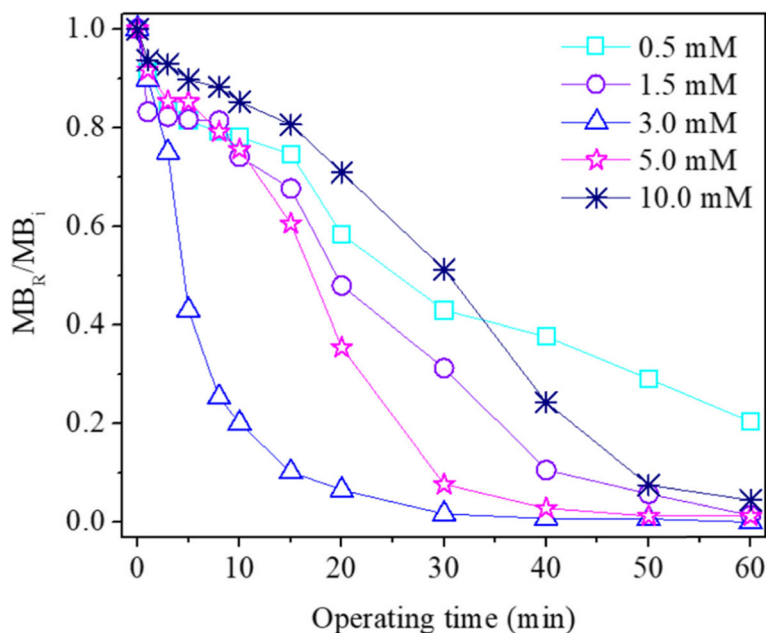


**Fig. 10** Effect of  $\text{H}_2\text{O}_2$  dosage on MB dye degradation by photo-Fenton-like system ( $[\text{MB}]_i = 0.06 \text{ mM}$ ;  $\text{pH}_i = 3.0$ ; cat. dosage =  $0.85 \text{ g L}^{-1}$ ; air flow rate =  $6 \times 10^{-3} \text{ m}^3 \text{ min}^{-1}$ ; UV = 365 nm)

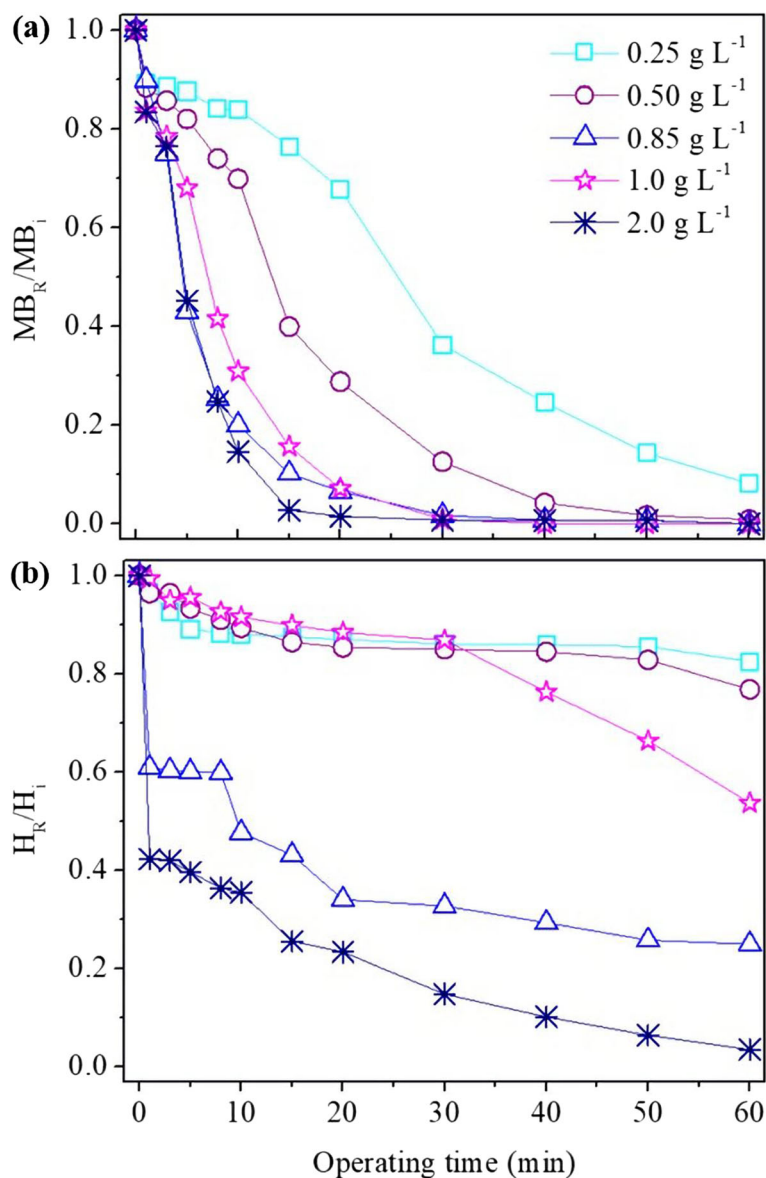


**Fig. 11** Effect of catalyst loading on MB dye degradation by photo-Fenton-like system ( $[MB]_i = 0.06 \text{ mM}$ ;  $[H_2O_2]_i = 3.0 \text{ mM}$ ;  $pH_i = 3.0$ ; air flow rate  $= 6 \times 10^{-3} \text{ m}^3 \text{ min}^{-1}$ ;  $UV = 365 \text{ nm}$ )

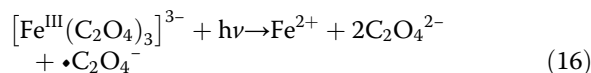
generated more  $\bullet OH$  radicals. Interestingly, at catalyst loading of  $1.0 \text{ g L}^{-1}$  the decoloration rate of MB was observed to be slightly slower than  $0.85 \text{ g L}^{-1}$  evidently at the first 15 min which could be affected by the  $H_2O_2$  consumption in the reaction system (Fig. 11b). The higher MB decoloration rate at a catalyst loading of  $0.85 \text{ g L}^{-1}$  was possibly achieved as result of higher consumption rate of  $H_2O_2$  leading to higher  $\bullet OH$  radical generation. Nonetheless, the optimum catalyst loading considered was  $1.0 \text{ g L}^{-1}$  due to lower  $H_2O_2$  concentration consumed at this condition which is more economical for the degradation process.

### 3.6 Evaluation of active species

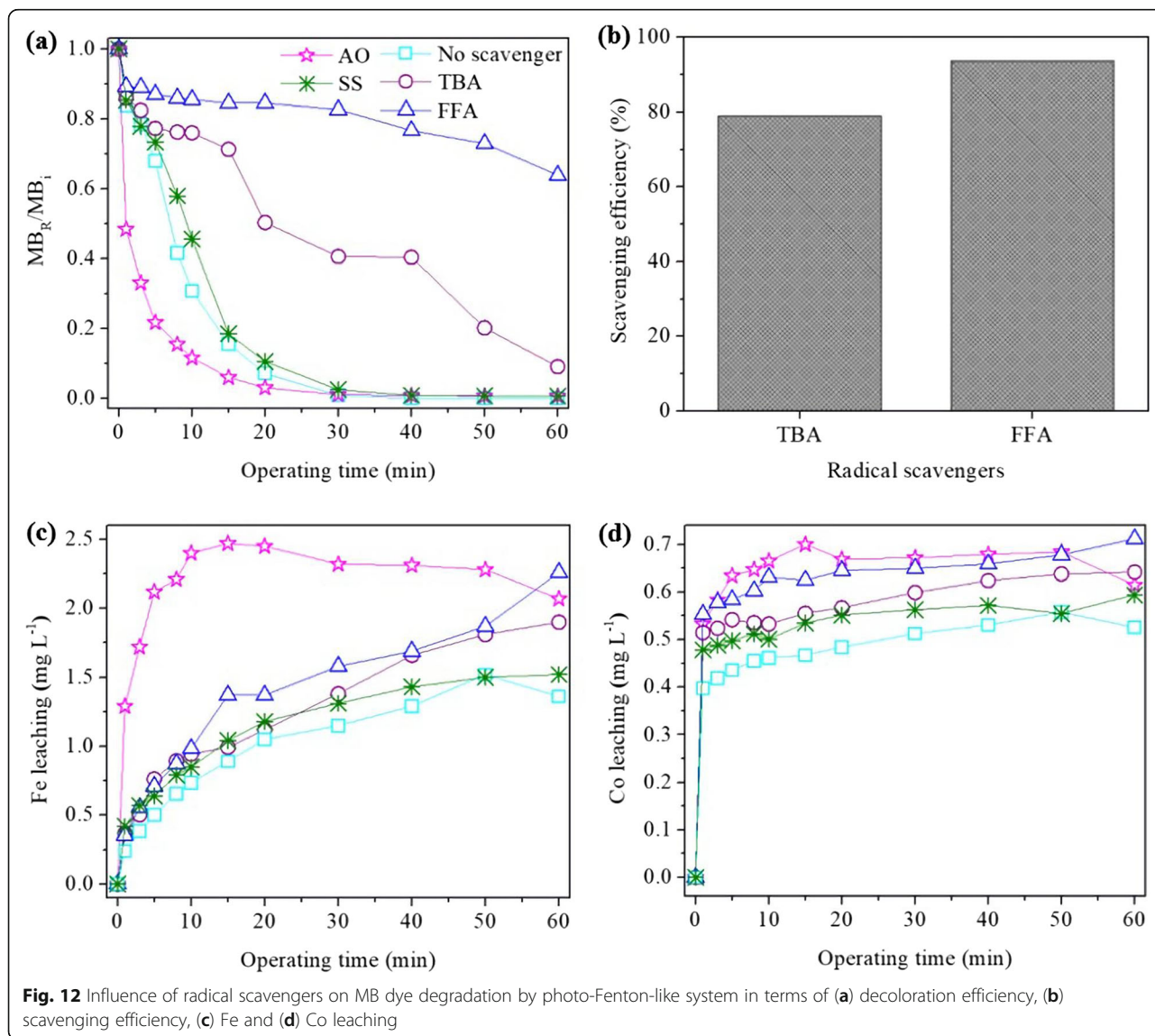
To determine the active species playing a critical role in the PFL process and to reveal the photodegradation mechanism of fFCS catalyst, radical quenching experiments were conducted to trap hydroxyl radical, superoxide radical, hole and electron. TBA was used as a model radical scavenger to determine the participation of  $\bullet OH$  radicals in MB degradation by PFL system using fFCS catalyst. Furthermore, FFA was selected for  $\bullet O_2^-$  radical trapping experiment. In addition to TBA and FFA, AO was chosen as  $h^+$  scavenger and SS was selected as  $e^-$  scavenger in the reaction system since electron-hole pairs are produced under light

illumination. As elucidated in Fig. 12a, adding SS unto the MB solution has a negligible effect on the PFL reaction, while on the contrary AO caused a quickening effect on the MB photodegradation efficiency. Conversely, Saleh and Traufik reported that the addition of AO on the sonophoto-Fenton process for the remediation of MB and CR using Fe<sub>3</sub>O<sub>4</sub>-ZnO/graphene nanocomposites decreased the degradation efficiency implying that holes play a very crucial role in the system [7]. In the present work, the acceleration in the MB degradation rate within 15 min with AO addition could be ascribed to the increase in iron and cobalt leaching at the first 15 min of operating time as indicated in Fig. 12c and d. Accordingly, the iron leached in the system possibly reacted with the oxalate ion from AO forming the photoactive complex, [Fe<sup>III</sup>(C<sub>2</sub>O<sub>4</sub>)<sub>3</sub>]<sup>3-</sup>, which was favorable for the

quick MB decoloration [46]. The mechanism can be described as follows through Eqs. (15)-(18):



In contrast, the decoloration efficiency dramatically reduced to 36% when FFA was used as a quencher with a scavenging efficiency of 94% (Fig. 12b). This is deemed to be essential for •O<sub>2</sub><sup>-</sup> radicals in the PFL response. Although 91% of MB was degraded when TBA existed in



the reaction system, it is evident in Fig. 8a that the rate of decoloration is much slower than that of the MB degradation without scavenger leading to a scavenging efficiency of 79%. These outcomes establish that  $\bullet\text{O}_2^-$  acts as the main oxidative species and  $\bullet\text{OH}$  also contributed to MB degradation by PFL reaction using fFCS catalyst.

### 3.7 Feasibility of industrial and engineering application

This study was performed on a laboratory scale under pre-determined operating conditions. Different catalyst preparation methods are used for Fe-Co catalyst synthesis used in the treatment of organic dyes including impregnation, sol-gel technique and hydrothermal method [10, 13, 14, 47]. Sun et al. synthesized Fe-Co/MCM-41 via hydrothermal method for 60 h at 140 °C [6]. Moreover, Fe-Co reached 66 h to be impregnated on PAM surface [13]. Fe-Co supported on  $\text{Al}_2\text{O}_3$ -MCM-41 was prepared by Pradhan et al. using a combination of sol-gel and hydrothermal methods at 120 °C for 24 h [14]. Likewise, hydrothermal method was utilized to synthesize Fe-Co/SBA-15 at 100 °C for 48 h [48]. The FBC technique used in this study was run for only 4 h under room temperature which reduced the synthesis time and operating temperature, and thus, leading to lesser energy consumption and operating cost. The synthesis time was reduced by about 83-94% and the operating temperature by 75-82%. For industrial and engineering application, this will be advantageous in terms of economic value. Catalyst cost is one of the critical considerations for successful catalyst development.

In terms of degradation efficiency, the catalytic performance of fFCS is comparable with the Fe-Co catalyst synthesized using the existing preparation methods. 25 mg L<sup>-1</sup> of Methyl Orange was reduced by 95% using hydrothermally-synthesized Fe-Co/MCM-41 catalyst using peroxydisulfate concentration of 0.075 mM and catalyst loading of 0.2 g L<sup>-1</sup> at pH 5.6 under room temperature [6]. Using Fe-Co/ $\text{Al}_2\text{O}_3$ -MCM-41 catalyst synthesized via sol-gel cum hydrothermal method in the PFL system, 100% MB degradation was achieved within 1 h under visible light [14]. Furthermore, 96% CR degradation was obtained with a degradation rate of 0.063 min<sup>-1</sup> at 35 °C within 1 h [13]. Besides, Cai et al. treated Orange II dye achieving 93% degradation within 2 h assisted by ultrasound irradiation [48]. In this work, complete degradation of MB was attained under PFL system within 1 h. It can be observed that the tested fFCS have comparable catalytic performance with the catalysts synthesized via existing synthesis techniques. With this, further work can be conducted to explore FBC as a novel method for bimetallic catalyst synthesis to provide improved activity and selectivity for catalytic reactions.

3P-FBR was used in this study which applies the principles of heterogeneous FBR-Fenton (FBF) process. Herein, the sufficient catalytic reaction sites are provided by the active carriers (catalyst particles) which also leads to high mass transfer rate induced by carrier fluidization caused by the air supplied to the reactor. At present, FBF process have been used on an industrial scale in Taiwan treating large volumes of persistent organic pollutant (POP) effluents from petrochemical and pulp and paper mill industries since 2002 yielding complete POP removal under continuous operation [47]. According to the results drawn in this work, PFL process using the 3P-FBR is an effective treatment for organic wastewater which can help improve the existing industrial FBF systems with the use of bimetallic catalysts. The application of the FBC-derived Fe-Co catalyst in the industrial and engineering field, however, presents current challenging issues such as improvement of mineralization efficiency which is significant on real case wastewater and reduction of metal leaching causing catalyst deactivation problem leading to lesser catalytic active sites. Strong metal-support interaction could also be studied and improved in relation to the leaching of iron and cobalt in the reaction system. Finally, the results in this work could provide useful information for bimetallic catalyst development and will stimulate further research activities in the field of heterogenous FBF process for possible industrial up-scale.

## 4 Conclusions

The Fe-Co/SiO<sub>2</sub> catalyst was successfully fabricated using the FBC process and this study is the first to investigate its catalytic activity and performance toward MB degradation and mineralization. The effects of initial pH, H<sub>2</sub>O<sub>2</sub> dosage, and catalyst loading were discussed thoroughly. The results indicate that 20 mg L<sup>-1</sup> of MB dye could be completely degraded via PFL process involving initial pH of 3.0, 3.0 mM of H<sub>2</sub>O<sub>2</sub> and 1.0 g L<sup>-1</sup> of fFCS catalyst under UV-A light irradiation. The FBC-derived catalyst presented a good catalytic activity toward MB dye. The catalytic performance of this catalyst is comparable with the impregnated catalyst. Based on the radical quenching experiment, the main reactive oxygen species were  $\bullet\text{O}_2^-$  and  $\bullet\text{OH}$  radicals. Although complete MB decoloration was achieved using fFCS catalyst, 65% mineralization efficiency demonstrated the existence of intermediates derived from the PFL process.

### Acknowledgements

The authors would like to thank the Ministry of Science and Technology, Taiwan. Special thanks to Ma. Antonette A. Rubios for her valuable insights into the work.

### Authors' contributions

Khyle Glainmer N. Quiton conceptualized the study and carried out the experimental studies. Ming-Chun Lu provided conceptual and technical

guidance for all the aspects of the work. Yao-Hui Huang commented, reviewed, and approved its completion. All authors read and approved the final manuscript.

### Funding

This work was supported by the Ministry of Science and Technology, Taiwan with grant no. MOST 107-2221-E-005-081-MY3 and MOST 106-2622-E006-037-CC2.

### Availability of data and materials

All data generated or analyzed in this study are available from the corresponding author on reasonable request.

### Declarations

#### Competing interests

The authors declare that they have no known competing financial interests.

#### Author details

<sup>1</sup>Department of Chemical Engineering, National Cheng Kung University, Tainan 701, Taiwan. <sup>2</sup>Department of Environmental Engineering, National Chung Hsing University, Taichung 40227, Taiwan.

Received: 25 October 2021 Accepted: 17 February 2022

Published online: 28 March 2022

### References

- Zhang YZ, Xiong XY, Han Y, Zhang XH, Shen F, Deng SH, et al. Photoelectrocatalytic degradation of recalcitrant organic pollutants using TiO<sub>2</sub> film electrodes: an overview. *Chemosphere*. 2012;88:145–54.
- Dalrymple RM, Carfagno AK, Sharpless CM. Correlations between dissolved organic matter optical properties and quantum yields of singlet oxygen and hydrogen peroxide. *Environ Sci Technol*. 2010;44:5824–9.
- Su SS, Liu YY, Liu XM, Jin W, Zhao YP. Transformation pathway and degradation mechanism of methylene blue through beta-FeOOH@GO catalyzed photo-Fenton-like system. *Chemosphere*. 2019;218:83–92.
- Tolba A, Alalm MG, Elsamadony M, Mostafa A, Afify H, Dionysiou DD. Modeling and optimization of heterogeneous Fenton-like and photo-Fenton processes using reusable Fe<sub>3</sub>O<sub>4</sub>-MWCNTs. *Process Saf Environ*. 2019;128:273–83.
- Liu YY, Jin W, Zhao YP, Zhang GS, Zhang W. Enhanced catalytic degradation of methylene blue by alpha-Fe<sub>2</sub>O<sub>3</sub>/graphene oxide via heterogeneous photo-Fenton reactions. *Appl Catal B-Environ*. 2017;206:642–52.
- Saleh R, Taufik A. Degradation of methylene blue and congo-red dyes using Fenton, photo-Fenton, sono-Fenton, and sonophoto-Fenton methods in the presence of iron (II/III) oxide/zinc oxide/graphene (Fe<sub>3</sub>O<sub>4</sub>/ZnO/graphene) composites. *Sep Purif Technol*. 2019;210:563–73.
- Koli PB, Kapadnis KH, Deshpande UG, Patil MR. Fabrication and characterization of pure and modified Co<sub>3</sub>O<sub>4</sub> nanocatalyst and their application for photocatalytic degradation of eosin blue dye: a comparative study. *J Nanostructure Chem*. 2018;8:453–63.
- Hou JF, He XD, Zhang SQ, Yu JL, Feng MB, Li XD. Recent advances in cobalt-activated sulfate radical-based advanced oxidation processes for water remediation: a review. *Sci Total Environ*. 2021;770:145311.
- Szegedi A, Popova M, Minchev C. Catalytic activity of Co/MCM-41 and Co/SBA-15 materials in toluene oxidation. *J Mater Sci*. 2009;44:6710–6.
- Sun XW, Xu DY, Dai P, Liu X, Tan F, Guo QJ. Efficient degradation of methyl orange in water via both radical and non-radical pathways using Fe-Co bimetal-doped MCM-41 as peroxymonosulfate activator. *Chem Eng J*. 2020;402.
- Yao YJ, Cai YM, Wu GD, Wei FY, Li XY, Chen H, et al. Sulfate radicals induced from peroxymonosulfate by cobalt manganese oxides (Co<sub>x</sub>Mn<sub>3-x</sub>O<sub>4</sub>) for Fenton-Like reaction in water. *J Hazard Mater*. 2015;296:128–37.
- Ding DH, Yang SJ, Chen LW, Cai TM. Degradation of norfloxacin by CoFe alloy nanoparticles encapsulated in nitrogen doped graphitic carbon (CoFe@N-GC) activated peroxymonosulfate. *Chem Eng J*. 2020;392:123725.
- Aftab TB, Hussain A, Li DX. Application of a novel bimetallic hydrogel based on iron and cobalt for the synergistic catalytic degradation of Congo Red dye. *J Chin Chem Soc-Taipei*. 2019;66:919–27.
- Pradhan AC, Sahoo MK, Bellamkonda S, Parida KM, Rao GR. Enhanced photodegradation of dyes and mixed dyes by heterogeneous mesoporous Co-Fe/Al<sub>2</sub>O<sub>3</sub>-MCM-41 nanocomposites: nanoparticles formation, semiconductor behavior and mesoporosity. *RSC Adv*. 2016;6:94263–77.
- Duan YY, Luo JM, Zhou SC, Mao XY, Shah MW, Wang F, et al. TiO<sub>2</sub>-supported Ag nanoclusters with enhanced visible light activity for the photocatalytic removal of NO. *Appl Catal B-Environ*. 2018;234:206–12.
- Yang Z, Zhang X, Pu SJ, Ni RX, Lin Y, Liu Y. Novel Fenton-like system (Mg/Fe-O<sub>2</sub>) for degradation of 4-chlorophenol. *Environ Pollut*. 2019;250:906–13.
- Priambodo R, Tan YL, Shih YJ, Huang YH. Fluidized-bed crystallization of iron phosphate from solution containing phosphorus. *J Taiwan Inst Chem E*. 2017;80:247–54.
- Su CC, Abarca RRM, de Luna MDG, Lu MC. Phosphate recovery from fluidized-bed wastewater by struvite crystallization technology. *J Taiwan Inst Chem E*. 2014;45:2395–402.
- Shih YJ, Huang RL, Huang YH. Adsorptive removal of arsenic using a novel akhtenskite coated waste goethite. *J Clean Prod*. 2015;87:897–905.
- Warmadewanthi, Liu JC. Selective precipitation of phosphate from semiconductor wastewater. *J Environ Eng*. 2009;135:1063–70.
- Forrest AL, Fattah KP, Mavinic DS, Koch FA. Optimizing struvite production for phosphate recovery in WWTP. *J Environ Eng-ASCE*. 2008;134:395–402.
- Taghavi-moghaddam J, Knowles GP, Chaffee AL. Preparation and characterization of mesoporous silica supported cobalt oxide as a catalyst for the oxidation of cyclohexanol. *J Mol Catal A-Chem*. 2012;358:79–88.
- Huang YY, Liu F, Li HD. Degradation of tetrachloromethane and tetrachloroethene by Ni/Fe bimetallic nanoparticles. *J Phys Conf Ser*. 2009;188:012014.
- Aluha J, Abatzoglou N. Gold-promoted plasma-synthesized Ni-Co-Fe/C catalyst for Fischer-Tropsch synthesis. *Gold Bull*. 2017;50:147–62.
- Uskokovic V, Drofenik M. Synthesis of materials within reverse micelles. *Surf Rev Lett*. 2005;12:239–77.
- Kim HE, Lee J, Lee H, Lee C. Synergistic effects of TiO<sub>2</sub> photocatalysis in combination with Fenton-like reactions on oxidation of organic compounds at circumneutral pH. *Appl Catal B-Environ*. 2012;115:219–24.
- Dukkanci M, Gunduz G, Yilmaz S, Yaman YC, Prikhod'ko RV, Stolyarova IV. Characterization and catalytic activity of CuFeZSM-5 catalysts for oxidative degradation of Rhodamine 6G in aqueous solutions. *Appl Catal B-Environ*. 2010;95:270–8.
- Quiton KGN, Lu MC, Huang YH. Synthesis and catalytic utilization of bimetallic systems for wastewater remediation: a review. *Chemosphere*. 2021;262:128371.
- Gautam RK, Rawat V, Banerjee S, Sanroman MA, Soni S, Singh SK, et al. Synthesis of bimetallic Fe-Zn nanoparticles and its application towards adsorptive removal of carcinogenic dye malachite green and Congo red in water. *J Mol Liq*. 2015;212:227–36.
- Das M, Mishra D, Maiti TK, Basak A, Pramanik P. Bio-functionalization of magnetite nanoparticles using an aminophosphonic acid coupling agent: new, ultradispersed, iron-oxide folate nanoconjugates for cancer-specific targeting. *Nanotechnology*. 2008;19:415101.
- Jiratova K, Perekrestov R, Dvorakova M, Balabanova J, Topka P, Kostejn M, et al. Cobalt oxide catalysts in the form of thin films prepared by magnetron sputtering on stainless-steel meshes: performance in ethanol oxidation. *Catalysts*. 2019;9:806.
- Dias FF, Oliveira AAS, Arcanjo AP, Moura FCC, Pacheco JGA. Residue-based iron catalyst for the degradation of textile dye via heterogeneous photo-Fenton. *Appl Catal B-Environ*. 2016;186:136–42.
- Farias MF, Domingos YS, Fernandes GJT, Castro FL, Fernandes VJ, Costa MJF, et al. Effect of acidity in the removal-degradation of benzene in water catalyzed by Co-MCM-41 in medium containing hydrogen peroxide. *Micropor Mesopor Mat*. 2018;258:33–40.
- Yang B, Tian Z, Zhang L, Guo YP, Yan SQ. Enhanced heterogeneous Fenton degradation of Methylene Blue by nanoscale zero valent iron (nZVI) assembled on magnetic Fe<sub>3</sub>O<sub>4</sub>/reduced graphene oxide. *J Water Process Eng*. 2015;5:101–11.
- Vinita M, Dorathi RPJ, Palanivelu K. Degradation of 2,4,6-trichlorophenol by photo Fenton's like method using nano heterogeneous catalytic ferric ion. *Sol Energy*. 2010;84:1613–8.
- Pignatello JJ, Oliveros E, Mackay A. Advanced oxidation processes for organic contaminant destruction based on the Fenton reaction and related chemistry. *Crit Rev Env Sci Tec*. 2006;36:1–84.
- De Laat J, Gallard H. Catalytic decomposition of hydrogen peroxide by Fe (III) in homogeneous aqueous solution: mechanism and kinetic modeling. *Environ Sci Technol*. 1999;33:2726–32.

38. Ahmed Y, Yaakob Z, Akhtar P. Degradation and mineralization of methylene blue using a heterogeneous photo-Fenton catalyst under visible and solar light irradiation. *Catal Sci Technol* 2016;6:1233–32.
39. Kosmulski M. pH-dependent surface charging and points of zero charge. IV. Update and new approach. *J Colloid Interf Sci.* 2009;337:439–48.
40. Arshadi M, Abdolmaleki MK, Mousavinia F, Khalafi-Nezhad A, Firouzabadi H, Gil A. Degradation of methyl orange by heterogeneous Fenton-like oxidation on a nano-organometallic compound in the presence of multi-walled carbon nanotubes. *Chem Eng Res Des.* 2016;112:113–21.
41. Kwon BG, Kim E, Lee JH. Pentachlorophenol decomposition by electron beam process enhanced in the presence of Fe (III)-EDTA. *Chemosphere.* 2009;74:1335–9.
42. Hu XB, Liu BZ, Deng YH, Chen HZ, Luo S, Sun C, et al. Adsorption and heterogeneous Fenton degradation of 17 $\alpha$ -methyltestosterone on nano Fe<sub>3</sub>O<sub>4</sub>/MWCNTs in aqueous solution. *Appl Catal B-Environ* 2011;107:274–83.
43. Guo XJ, Li HR, Zhao SG. Fast degradation of Acid Orange II by bicarbonate-activated hydrogen peroxide with a magnetic S-modified CoFe<sub>2</sub>O<sub>4</sub> catalyst. *J Taiwan Inst Chem E.* 2015;55:90–100.
44. An JJ, Zhu LH, Zhang YY, Tang HQ. Efficient visible light photo-Fenton-like degradation of organic pollutants using in situ surface-modified BiFeO<sub>3</sub> as a catalyst. *J Environ Sci-China.* 2013;25:1213–25.
45. Tbesi I, Benito M, Llorca J, Molins E, Sayadi S, Najjar W. Silver and manganese co-doped titanium oxide aerogel for effective diclofenac degradation under UV-A light irradiation. *J Alloy Compd.* 2019;779:314–25.
46. Xiao C, Li S, Yi FH, Zhang B, Chen D, Zhang Y, et al. Enhancement of photo-Fenton catalytic activity with the assistance of oxalic acid on the kaolin-FeOOH system for the degradation of organic dyes. *RSC Adv.* 2020;10:18704–14.
47. Garcia-Segura S, Bellotindos LM, Huang YH, Brillas E, Lu MC. Fluidized-bed Fenton process as alternative wastewater treatment technology – a review. *J Taiwan Inst Chem E.* 2016;67:211–25.
48. Cai C, Zhang H, Zhong X, Hou LW. Ultrasound enhanced heterogeneous activation of peroxymonosulfate by a bimetallic Fe-Co/SBA-15 catalyst for the degradation of Orange II in water. *J Hazard Mater.* 2015;283:70–9.

## Publisher's Note

Springer Nature remains neutral with regard to jurisdictional claims in published maps and institutional affiliations.

**Ready to submit your research? Choose BMC and benefit from:**

- fast, convenient online submission
- thorough peer review by experienced researchers in your field
- rapid publication on acceptance
- support for research data, including large and complex data types
- gold Open Access which fosters wider collaboration and increased citations
- maximum visibility for your research: over 100M website views per year

**At BMC, research is always in progress.**

Learn more [biomedcentral.com/submissions](https://biomedcentral.com/submissions)

